

Learning a Fourier Transform for Linear Relative Positional Encodings in Transformers

Krzysztof Choromanski ^{*1,2} Shanda Li ^{*3} Valerii Likhoshesterov ⁴ Avinava Dubey ¹
 Shengjie Luo ⁵ Di He ⁵ Yiming Yang ³ Tamas Sarlos ¹ Thomas Weingarten ¹ Adrian Weller ^{4,6}

Abstract

We propose a new class of linear Transformers called FourierLearner-Transformers (FLTs), which incorporate a wide range of relative positional encoding mechanisms (RPEs). These include regular RPE techniques applied for nongeometric data, as well as novel RPEs operating on the sequences of tokens embedded in higher-dimensional Euclidean spaces (e.g. point clouds). FLTs construct the optimal RPE mechanism implicitly by learning its spectral representation. As opposed to other architectures combining efficient low-rank linear attention with RPEs, FLTs remain practical in terms of their memory usage and do not require additional assumptions about the structure of the RPE-mask. FLTs allow also for applying certain structural inductive bias techniques to specify masking strategies, e.g. they provide a way to learn the so-called *local RPEs* introduced in this paper and providing accuracy gains as compared with several other linear Transformers for language modeling. We also thoroughly tested FLTs on other data modalities and tasks, such as: image classification and 3D molecular modeling. For 3D-data FLTs are, to the best of our knowledge, the first Transformers architectures providing RPE-enhanced linear attention.

1. Introduction

Transformers architectures have revolutionized machine learning (ML), not only by providing significant quantitative gains of ML models, but by leading to dramatic qualitative improvements and opening new opportunities for applying them in few- or even zero-shot learning and abstract reasoning settings (Chowdhery et al., 2022; Brown et al., 2020;

Radford & Narasimhan, 2018; Ramesh et al., 2021; Reed et al., 2022; Ouyang et al., 2022; Srivastava et al., 2022; Lewkowycz et al., 2022; Rae et al., 2021; Borgeaud et al., 2022; Devlin et al., 2019; Raffel et al., 2020; Liu et al., 2019; Lan et al., 2020; Du et al., 2022; Thoppilan et al., 2022).

The research on scaling up the attention architecture, a core module of Transformers responsible for direct propagation of the signal between different tokens of the input sequence, started with their birth (Vaswani et al., 2017). Attention modules have quadratic space and time complexity with respect to the input sequence length L and thus are computationally incapable of modeling longer-range distances in long input sequences. The research on “efficient” Transformers has taken on a new importance as the size of Transformers models grew from the GPT-1 architecture of “only” **117M** parameters to GPT-3 with **175B** parameters, a **1000 \times** increase within just two years.

In several applications, *local attention* (Vaswani et al., 2021a; Zhou et al., 2021) addresses these new challenges. Tokens attend only to the compact sets of their neighbors, and the attention matrix is effectively zeroed out in most entries. In other problems requiring direct modeling of long-range dependencies, this approach is not sufficient (Zaheer et al., 2020). For instance, genome modeling (Gupta & Rush, 2017; Ji et al., 2021; Clauwaert et al., 2021) is a notoriously difficult task, because several of the DNA’s functionalities, such as regulatory properties, depend directly on the DNA’s 3D conformation and thus are inherently non-local phenomena.

To model long-range dependencies directly, several other models were proposed, where tokens were grouped together into subsets via clustering or hashing methods (Roy et al., 2021; Vyas et al., 2020; Kitaev et al., 2020; Sun et al., 2022). The attention was then modeled only for pairs of tokens within the same partition. In these approaches, the resulting attention matrices are still sparse.

Another popular class of scalable Transformers architectures, called *Performers*, was proposed by Choromanski et al. (2021). The idea is to find an approximate low-rank decomposition of the attention matrix and leverage it to improve space and time complexity of the attention mecha-

^{*}Equal contribution ¹Google Research ²Columbia University
³Carnegie Mellon University ⁴University of Cambridge ⁵Peking University ⁶The Alan Turing Institute. Correspondence to: Krzysztof Choromanski <kchoro@google.com>.

nism via the associativity property of matrix multiplications. Interestingly, in contrast to previously discussed methods, the approximate attention matrix (that is never explicitly constructed, but rather used implicitly) is an unbiased estimate of the original attention matrix encoding similarities between tokens via the softmax-kernel. The random feature map mechanism used in Performers to produce the low-rank decomposition of the softmax attention matrix was the subject of significant follow-up research (Choromanski et al., 2022b; Likhoshesterov et al., 2022; Chowdhury et al., 2022). Several other kernels for replacing softmax attention upon their effective linearization, such as Performer-ReLU, were studied. Furthermore, as they are straightforward to implement, Performers were adopted into many Transformers stacks to provide linear space and time complexity (Yuan et al., 2021; Horn et al., 2021; Tay et al., 2021) – recently even for robotic navigation (Xiao et al., 2022).

Unfortunately this simplicity comes at a price. It is well known that incorporating structural inductive priors – which is usually implemented via various additive relative masking mechanisms in regular attention architectures – is difficult for Performers. We refer to these methods as *Relative Positional Encodings* (or RPEs) (Shaw et al., 2018; Raffel et al., 2020; Wu et al., 2021; Gong et al., 2022; Luo et al., 2022b). RPEs play a critical role in improving the performance of Transformers in long-range modeling, e.g. for speech (Liutkus et al., 2021) and genomic data (Ziga Avsec et al., 2021).

At first glance, Performers are not compatible with general RPE techniques, since they seem to require explicit materialization of the attention matrix to apply the RPE-mask, which is exactly what Performers avoid in order to achieve computational improvements.¹ Recently a substantial effort was made to reconcile Performers with RPEs (more details in Sec. 2), but so far these attempts fell short of providing two properties at the same time: (a) practical computational gains, and (b) inclusion of general RPE methods, for inputs with nontrivial topological structures.

In this paper, we propose a new class of linear Transformers called FourierLearner-Transformers (FLTs), which incorporate a wide range of relative positional encoding mechanisms (RPEs). These include regular RPE techniques applied for nongeometric data, and novel RPEs operating on sequences of tokens embedded in higher-dimensional Euclidean spaces (e.g. point clouds). FLTs construct the optimal RPE mechanism implicitly by learning its spectral representation. As opposed to other architectures combining

¹Certain RPE masking mechanisms can be implemented in linear space and time complexity, for instance *causal masking* that can be thought of as an instantiation of RPE and admits linear incorporation into Performers via the *prefix-sum* mechanism, see (Choromanski et al., 2021).

efficient low-rank linear attention with RPEs, FLTs remain practical in terms of their memory usage and do not require additional assumptions about the structure of the RPE-mask. FLTs also allow the application of certain structural inductive bias techniques to specify masking strategies, e.g. they provide a way to learn what we call *local RPEs*, introduced in this paper and providing accuracy gains compared with several other linear Transformers for language modeling. We thoroughly test FLTs on other data modalities and tasks, such as image classification and molecular modeling. For 3D-data FLTs are, to the best of our knowledge, the first Transformers architectures providing linear attention and incorporating RPE-masking.

To summarize, our main contributions are as follows:

1. In Sec. 3, we introduce the RPE-enhanced linear attention defining FourierLearner-Transformers. We discuss several instantiations (see Sec. 3.3), in particular FLTs with so-called *Gaussian mixture RPEs*, *shift-invariant kernel RPEs* and *local RPEs*.
2. In Sec. 4, we conduct extensive empirical evaluations of FLTs on tasks ranging from language modeling (Sec. 4.1), through image classification (Sec. 4.2) to molecular property predictions (Sec. 4.3). We show in particular that FLTs obtain the most accurate language models compared to **nine** other strong scalable Transformer architectures, with the local RPE variant introduced in this paper achieving the best performance.

2. Related works

One of the first attempts to address the problem of combining low-rank implicit attention Transformers with RPEs was presented in (Liutkus et al., 2021). The method relies on the low-rank decomposition of the RPE-mask and comes in two variants: sineSPE (also in a gated form) and convSPE. Both model the RPE-mask as a stationary position kernel with a Toeplitz mask structure. While sineSPE represents the values of the kernel via periodic functions with a fixed number of sinusoidal components, convSPE uses convolutions and random projections.

The time complexity of the two variants are $O(drLT^2)$ and $O(drLP)$ respectively, where d is query/key dimensionality, r is the number of rows of the random noise (projection) matrices, L is the sequence length, T stands for the number of sinusoidal components and P is the convolutional filters' lengths. While linear in L , in practice these mechanisms need to be used with sufficiently small T and P to satisfy computational demands, and effectively achieved 7 points worse perplexity on language modeling tasks compared to FLTs (see Sec. 4.1). They also constrain the RPE-mask to be a valid kernel-matrix, which need not to be the case (for instance, the causal mechanism can be considered an

RPE masking method but does not even provide a symmetric RPE-mask). Finally, they cannot be applied for even more general RPE mechanisms with tokens embedded in the higher-dimensional Euclidean spaces.

More recently, Luo et al. (2021) showed that the RPE mechanism for 1D sequential data (e.g., language sequences) can be combined with Performers in $O(L \log(L))$ time complexity. The method relies on the elegant observation that log-linear time complexity can be achieved as long as the exponentiated RPE-mask supports fast matrix-vector multiplication, and that this is the case for the RPEs defined in 1D since the corresponding masks have a Toeplitz structure. Interestingly, the algorithm does not even approximate the RPE mechanism, but applies its exact variant. Unfortunately, the space complexity of the method is $O(Lmd)$, where m stands for the number of kernel features and L and d are as before. Even though still linear in L , it is now much larger than for the corresponding Performer variant ($O(Lm + md + Ld)$). In our experiments, this variant worked well for language modeling (see Sec. 4.1), but ran out of memory for image classification tasks (see Sec. 4.2).

Even more recently, this algorithm has been extended to the substantially more general RPE mechanisms, enabling high-dimensional spaces for positional vectors, and leveraging a large class of methods for efficient matrix-vector multiplication for the exponentiated RPE-mask matrix (Choromanski et al., 2022a). Though providing a comprehensive support for the general RPE mechanism, this method is still characterized by $O(Lmd)$ space complexity, which becomes a computational bottleneck unless a sufficiently small number of kernel features m is used.

3. The algorithm

3.1. Preliminaries

We start by introducing the general relative positional encoding (RPE) mechanism in Transformers, and regular RPE-free Performer architectures.

Consider an input sequence of L tokens. The attention used in a regular Transformer linearly projects their representations: $\mathbf{x}_1, \dots, \mathbf{x}_L \in \mathbb{R}^N$ into three learnable matrices $\mathbf{Q}, \mathbf{K} \in \mathbb{R}^{N \times d_{QK}}$, $\mathbf{V} \in \mathbb{R}^{N \times d_V}$ called *queries*, *keys* and *values* respectively. We also associate with all the tokens additional feature vectors $\mathbf{r}_1, \dots, \mathbf{r}_L \in \mathbb{R}^\ell$ that are used to define the RPE mechanism, see below.

Definition 3.1 (General RPE for attention). *General Relative Positional Encoding* enhanced attention is of the following form, where $\mathbf{N} = [f(\mathbf{r}_i - \mathbf{r}_j)]_{i,j=1,\dots,L} \in \mathbb{R}^{L \times L}$ is the so-called *RPE-mask* and $f: \mathbb{R}^\ell \rightarrow \mathbb{R}$ is a (potentially learnable) function:

$$\text{Att}(\mathbf{Q}, \mathbf{K}, \mathbf{V}, \mathbf{N}) = \mathbf{D}^{-1} \mathbf{A} \mathbf{V},$$

$$\mathbf{A} = \exp \left(\mathbf{N} + \frac{\mathbf{Q} \mathbf{K}^\top}{\sqrt{d_{QK}}} \right), \quad \mathbf{D} = \text{diag}(\mathbf{A} \mathbf{1}_L). \quad (1)$$

Here $\exp(\cdot)$ is applied element-wise, $\mathbf{1}_L$ is the all-one vector of length L , and $\text{diag}(\cdot)$ is a diagonal matrix with the input vector as the diagonal. The time complexity of computing Eq. (1) is $O(L^2 d)$.

Low-rank attention techniques leverage a decomposition of the attention matrix \mathbf{A} to avoid the quadratic space and time complexity in L by avoiding explicit materialization of \mathbf{A} . For the softmax attention, this is achieved by linearizing the softmax-kernel $K(\mathbf{x}, \mathbf{y}) \stackrel{\text{def}}{=} \exp(\mathbf{x}^\top \mathbf{y})$ via novel random features mechanisms: $K(\mathbf{x}, \mathbf{y}) = \mathbb{E}[\phi(\mathbf{x})^\top \phi(\mathbf{y})]$ for certain randomized mappings: $\phi: \mathbb{R}^{d_{QK}} \rightarrow \mathbb{R}^m$ (and some $m \in \mathbb{N}^*$). This mechanism leads to the fruitful class of linear space and time complexity Transformers, called Performers (Choromanski et al., 2021). We refer to vector $\phi(\mathbf{u})$ as a *random feature map* (RFM) for $\mathbf{u} \in \mathbb{R}^{d_{QK}}$. We then define $\mathbf{Q}', \mathbf{K}' \in \mathbb{R}^{L \times m}$ as matrices of rows given as $\phi(\mathbf{q}_i^\top d_{QK}^{-\frac{1}{4}})^\top$ and $\phi(\mathbf{k}_i^\top d_{QK}^{-\frac{1}{4}})^\top$ respectively. The softmax-kernel linearization with no RPE-masking directly leads to the following approximate algorithm for attention:

$$\widehat{\text{Att}}_{\mathbf{K}}(\mathbf{Q}, \mathbf{K}, \mathbf{V}) = \widehat{\mathbf{D}}^{-1} (\mathbf{Q}'((\mathbf{K}')^\top \mathbf{V})), \quad (2)$$

$$\widehat{\mathbf{D}} = \text{diag}(\mathbf{Q}'((\mathbf{K}')^\top \mathbf{1}_L)).$$

Here $\widehat{\text{Att}}_{\mathbf{K}}$ stands for the approximate attention and brackets indicate the order of computations. The time and space complexity of this mechanism are $O(Lmd)$ and $O(Lm + md + Ld)$ respectively, compared to $O(L^2 d)$ and $O(L^2 + Ld)$ for regular attention. Thus for $m \ll L$, Performers provide substantial computational improvements.

3.2. The FourierLearner-Transformer (FLT)

The algorithm presented in Eq. (2) does not incorporate RPE mechanisms. However, any low rank decomposition of the RPE-mask \mathbf{N} from Eq. (1) would naturally lead to a Performer-friendly RPE attention mechanism. Indeed, the following is true if $\widehat{\mathbf{N}} = \mathbf{N}_1 \mathbf{N}_2^\top$ for $\mathbf{N}_1, \mathbf{N}_2 \in \mathbb{R}^{L \times r}$:

$$\widehat{\mathbf{A}} \stackrel{\text{def}}{=} \exp \left(\widehat{\mathbf{N}} + \frac{\mathbf{Q} \mathbf{K}^\top}{\sqrt{d_{QK}}} \right) = \exp \left(\widehat{\mathbf{Q}} \widehat{\mathbf{K}}^\top \right), \quad (3)$$

and $\widehat{\mathbf{Q}} = [\mathbf{N}_1, \mathbf{Q} d_{QK}^{-\frac{1}{4}}] \in \mathbb{R}^{L \times (m+r)}$, $\widehat{\mathbf{K}} = [\mathbf{N}_2, \mathbf{K} d_{QK}^{-\frac{1}{4}}] \in \mathbb{R}^{L \times (m+r)}$ where the concatenation is conducted along the second axis. RPE-masked attention is now translated to regular softmax attention that admits “Performization”, as described in Eq. (2). The time and space complexity of this mechanism are: $O(L(m+r)d)$ and $O(L(m+r) + (m+r)d + Ld)$ respectively. Below we explain how the decomposition of \mathbf{N} into \mathbf{N}_1 and \mathbf{N}_2 is conducted.

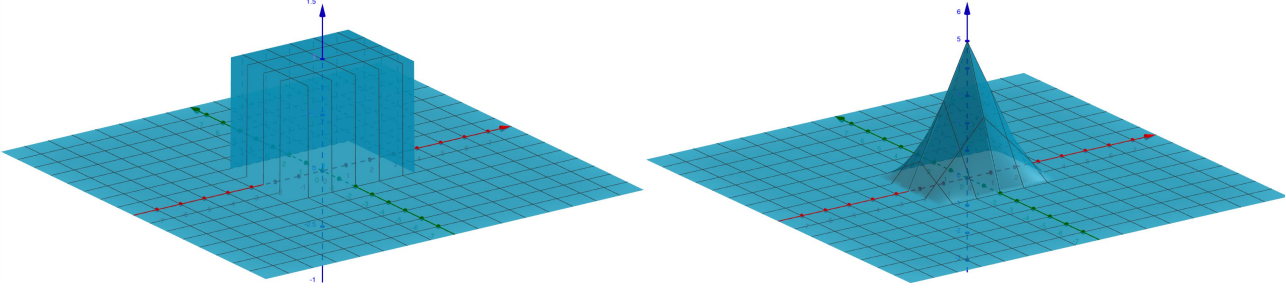


Figure 1. Examples of the local RPE mechanisms discussed in Sec. 3.3 and supported via FLTs. Both examples are for tokens with positions described by two coordinates ($\ell = 2$). The x and y coordinates encode the difference vector $\Delta \mathbf{r} = (\Delta r_1, \Delta r_2)^\top$. The z -coordinate provides the value of a function f . **Left:** Non-continuous local RPE mechanism for $\ell = 2$ of the form: $f_{\mathbf{v}, C}(\Delta \mathbf{r}) = C \cdot \mathbb{1}[|\Delta r_1| \leq v_1] \mathbb{1}[|\Delta r_2| \leq v_2]$ for some $\mathbf{v} = (v_1, v_2)^\top$. **Right:** This time $f_{\mathbf{v}}(\Delta \mathbf{r}) = \mathbb{1}[|\Delta r_1| \leq v_1] \mathbb{1}[|\Delta r_2| \leq v_2](-|\Delta r_1| + v_1)(-|\Delta r_2| + v_2)$. The latter local RPE mechanism is continuous, but as the former, vanishes outside the bounded region. Both can be modeled with FLTs via FTs, factorized into powers of sinc functions $\frac{\sin(\pi x)}{\pi x}$.

The key observation is that the function $f : \mathbb{R}^\ell \rightarrow \mathbb{R}$ can be rewritten as follows, where $g : \mathbb{R}^\ell \rightarrow \mathbb{R}$ denotes its Fourier Transform (FT):

$$f(\mathbf{z}) = \int_{\mathbb{R}^\ell} \exp(2\pi i \mathbf{z}^\top \boldsymbol{\xi}) \frac{g(\boldsymbol{\xi})}{p(\boldsymbol{\xi})} p(\boldsymbol{\xi}) d\boldsymbol{\xi}. \quad (4)$$

Here $i^2 = -1$ and p is the probability density function of some probabilistic distribution $P \in \mathcal{P}(\mathbb{R}^\ell)$. The representation from Eq. (4) leads to the following RFM-mechanism for unbiased approximation of $f(\mathbf{x} - \mathbf{y})$ for any $\mathbf{x}, \mathbf{y} \in \mathbb{R}^\ell$, where m stands for the number of random features:

$$f(\mathbf{x} - \mathbf{y}) = \mathbb{E}[\varphi(\mathbf{x})^\top \psi(\mathbf{y})]. \quad (5)$$

The random feature maps $\varphi, \psi : \mathbb{R}^\ell \rightarrow \mathbb{R}^r$ are defined as follows for $\boldsymbol{\xi}_1, \dots, \boldsymbol{\xi}_r \stackrel{\text{iid}}{\sim} P$, $\hat{\boldsymbol{\xi}}_j = -\boldsymbol{\xi}_j$, and $t_j u_j = 1$ for $j = 1, \dots, r$:

$$\begin{aligned} \varphi(\mathbf{z}) &\stackrel{\text{def}}{=} \frac{1}{\sqrt{r}} \left(e^{2\pi i \mathbf{z}^\top \boldsymbol{\xi}_1} \sqrt{\frac{g(\boldsymbol{\xi}_1)}{p(\boldsymbol{\xi}_1)}} t_1, \dots, e^{2\pi i \mathbf{z}^\top \boldsymbol{\xi}_r} \sqrt{\frac{g(\boldsymbol{\xi}_r)}{p(\boldsymbol{\xi}_r)}} t_r \right)^\top \\ \psi(\mathbf{z}) &\stackrel{\text{def}}{=} \frac{1}{\sqrt{r}} \left(e^{2\pi i \mathbf{z}^\top \hat{\boldsymbol{\xi}}_1} \sqrt{\frac{g(\boldsymbol{\xi}_1)}{p(\boldsymbol{\xi}_1)}} u_1, \dots, e^{2\pi i \mathbf{z}^\top \hat{\boldsymbol{\xi}}_r} \sqrt{\frac{g(\boldsymbol{\xi}_r)}{p(\boldsymbol{\xi}_r)}} u_r \right)^\top \end{aligned}$$

Then, we can define $\mathbf{N}_1 = [\varphi(\mathbf{x}_1), \dots, \varphi(\mathbf{x}_L)]^\top \in \mathbb{R}^{L \times r}$ and $\mathbf{N}_2 = [\psi(\mathbf{x}_1), \dots, \psi(\mathbf{x}_L)]^\top \in \mathbb{R}^{L \times r}$, respectively.

Instead of learning function f and trying to compute its Fourier Transform g to obtain a low-rank decomposition of \mathbf{N} , the FourierLearner-Transformer (FLT) directly learns g , effectively learning an implicit representation of f . In practice, P needs to be chosen in such a way that we can efficiently sample from it and compute its probability density function (e.g. Gaussian or truncated Gaussian distribution).

We point out that our formulations are general enough to cover a wide range of RPE variants used in practice.

Regular RPE for sequential data: In this setting the input sequence does not have richer geometric structure and thus vectors \mathbf{r}_j can be identified with the indices of tokens in the sequence, i.e., $\mathbf{r}_j = j$. Thus, FLT learns a function $g : \mathbb{R} \rightarrow \mathbb{R}$ (see: Sec. 4.1, 4.2).

RPE for the 3D-data: For this input type (e.g. point clouds or 3D molecular data), it is natural to identify vectors \mathbf{r}_j with the 3D coordinates of tokens. Therefore, FLT learns a function $g : \mathbb{R}^3 \rightarrow \mathbb{R}$ (see: Sec. 4.3).

Nowhere in the analysis so far have we relied on any structural properties of f . In particular, the matrix \mathbf{N} does not need to be a valid positive definite kernel-matrix or even symmetric. However, if needed, desired inductive bias can be incorporated into FLT via certain parameterization schemes used to train g , as we discuss next.

3.3. The topology of the Fourier Transform g

Gaussian mixture RPEs. One of the most general parameterizations of g that we have considered is the so-called *Gaussian mixture* variant:

$$g(\boldsymbol{\xi}) = \sum_{t=1}^T w_t \exp\left(-\frac{\|\boldsymbol{\xi} - \boldsymbol{\mu}_t\|^2}{2\sigma_t^2}\right). \quad (6)$$

Therefore the FT g is parameterized by $(2 + \ell)T$ numbers: $w_1, \dots, w_T, \sigma_1, \dots, \sigma_T \in \mathbb{R}$, $\boldsymbol{\mu}_1, \dots, \boldsymbol{\mu}_T \in \mathbb{R}^\ell$. In the special case where $T = 1$, the FT becomes a renormalized Gaussian kernel and as such, defines f as another Gaussian kernel.

Shift-invariant kernels for RPE-masks. It is straightforward to apply the FLT mechanism for RPEs to make \mathbf{N} a kernel-matrix of any *shift-invariant* kernel (Rahimi & Recht, 2007). Note that by Bochner's Theorem:

$$K(\mathbf{x} - \mathbf{y}) = C \int_{\mathbb{R}^\ell} e^{i(\mathbf{x} - \mathbf{y})^\top \boldsymbol{\xi}} p_K(\boldsymbol{\xi}) d\boldsymbol{\xi} \quad (7)$$

for the shift-invariant kernel: $K : \mathbb{R}^\ell \times \mathbb{R}^\ell \rightarrow \mathbb{R}$, the corresponding probabilistic distribution p_K and some positive constant $C > 0$. Thus to unbiasedly approximate an RPE-mask \mathbf{N} representing kernel-matrix $[K(\mathbf{s}_i, \mathbf{s}_k)]_{i,k=1,\dots,L}$ for the shift-invariant kernel K , it suffices to take: $\mathbf{r}_j = \frac{1}{2\pi} \mathbf{s}_j$, $g(\xi) = C p_K(\xi)$, and $t_j = u_j = 1$ for $j = 1, \dots, r$. Even if a particular class of shift-invariant kernels has been chosen, FLT still provides a way to learn its specific instantiation through learning an appropriately parameterized g .

Local RPEs. FLT is also capable (through the corresponding structured parameterized Fourier Transforms g) of modeling various schemes where the RPE mechanism needs to be applied only locally and regular attention is to be used for tokens far enough from each other. We call such strategies *local RPEs* or LRPEs. These include higher-dimensional LRPEs, particularly relevant for tokens with positions embedded in \mathbb{R}^ℓ for $\ell > 1$. The mechanism, which we present below in detail, can be considered an RFM-based smoothing of the original objective described by discrete parameters (such as the *radius of the local RPE* measured in the number of the nearest tokens).

The most basic LRPE type takes $\mathbf{r}_j = j$ and defines f as follows for an attention radius $v > 0$ and constant $C \in \mathbb{R}$:

$$f_{v,C}(\Delta r) = C \cdot \mathbb{1}[|\Delta r| \leq v]. \quad (8)$$

Such an RPE mechanism would (de)amplify the regular attention score between tokens close to each other by a certain multiplicative amount and might play a similar role as local attention (Vaswani et al., 2021b). It turns out that the FT for such a f has a particularly simple form:

$$g_{f_{v,C}}(\xi) = C \cdot \frac{\sin(2\pi v \xi)}{\pi \xi}. \quad (9)$$

Instead of using one indicator function in Eq. (8), one can also apply a sum of many with learnable radii and a list of coefficients C . Interestingly, RPEs from Eq. (8) can be easily generalized to a higher-dimensional LRPE of the following form (with \mathbf{r}_j in the formula for \mathbf{N} corresponding to positions of tokens in the higher-dimensional space \mathbb{R}^ℓ):

$$f_{\mathbf{v},C}(\Delta \mathbf{r}) = \prod_{j=1}^{\ell} C \cdot \mathbb{1}[|\Delta r_j| \leq v_j]. \quad (10)$$

The corresponding FT g can be factorized as follows:

$$g_{f_{\mathbf{v},C}}(\xi) = C \cdot \prod_{j=1}^{\ell} \frac{\sin(2\pi v_j \xi_j)}{\pi \xi_j}. \quad (11)$$

This result can be further generalized. The inverse FTs for functions g of the following form:

$$g_{k_1, \dots, k_\ell}^{v_1, \dots, v_\ell}(\xi) = C \cdot \prod_{j=1}^{\ell} \frac{\sin^{k_j}(2\pi v_j \xi_j)}{\pi \xi_j} \quad (12)$$

Model	Perplexity
Linear Trans. (Katharopoulos et al., 2020)	38.4
RFA-Gaussian (Peng et al., 2021)	33.6
RFA-arccos (Peng et al., 2021)	36.0
RFA-GATE-Gaussian (Peng et al., 2021)	31.3
RFA-GATE-arccos (Peng et al., 2021)	32.8
Performer (Choromanski et al., 2021)	31.1
Performer-sineSPE (Liutkus et al., 2021)	38.0
Performer-convSPE (Liutkus et al., 2021)	37.8
Log-linear Performer (Luo et al., 2021)	30.6
FLT (Gaussian mixture RPE) (ours)	30.3
FLT (local RPE) (ours)	30.1

Table 1. Language model perplexity scores on the WikiText-103 validation set. We highlight in **bold** the lowest perplexity.

are of the form: $f(\Delta \mathbf{r}) = M \cdot \prod_{j=1}^d f_j^{v_j}(\Delta r_j)$, where M is a constant and each $f_j^{v_j}$ is: (1) continuous, (2) symmetric, (3) with compact support of length depending on v_j , and (4) piece-wise a polynomial of order $k_j - 1$. Such functions f are natural candidates for continuous LRPE mechanisms for tokens with positions embedded in \mathbb{R}^ℓ and any $\ell \geq 1$. Examples of local RPE variants for $\ell = 2$, supported via FLT, are presented in Fig. 1.

The above theoretical results can be directly obtained via straightforward integration and a realization that the N -dim FT of a function: $h(x_1, \dots, x_N) \stackrel{\text{def}}{=} h_1(x_1) \cdot \dots \cdot h_N(x_N)$ can be represented as the product of 1D FTs of the individual components h_j .

4. Experiments

In this section, we provide experimental results on diverse tasks from language modeling, through image classification to molecular property prediction, to demonstrate the effectiveness of the FLT architecture.

4.1. Language modeling

We conduct experiments on the WikiText-103 language modeling task to show the effectiveness of our proposed method in NLP applications.

4.1.1. COMPARED METHODS

In this experiment, we study FLT with two RPE variants, Gaussian mixture RPE and local RPE. We compare our model with the following strong baselines:

- *Linear Transformer* proposed by Katharopoulos et al. (2020), which uses kernelized low-rank attention with $\text{elu}(\cdot) + 1$ as the feature map.

Dataset name	# of classes	Training set size	Test set size
ImageNet2012 (Deng et al., 2009)	1K	1.2M	100K
Places365 (Zhou et al., 2018)	365	1.8M	328K
I_naturalist2021 (Horn et al., 2018)	10K	2.7M	500K
Fashion-MNIST (Xiao et al., 2017)	10	60K	10K

Table 2. Details of the datasets used in image classification tasks with the FourierLearner-Transformer.

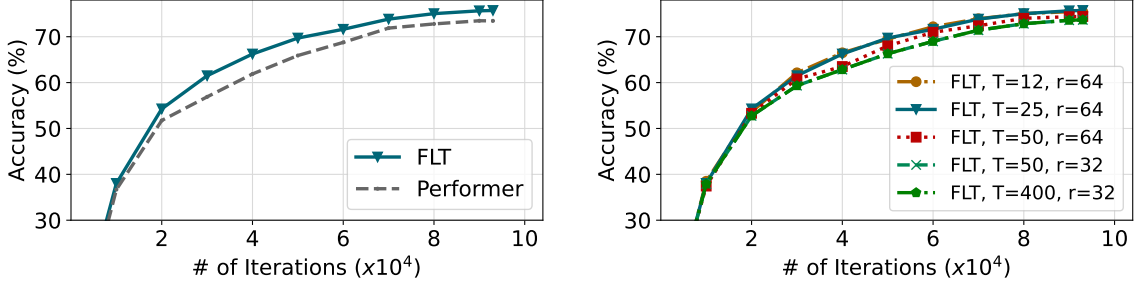


Figure 2. **Left:** Comparison of the FLT with a regular Performer on the ImageNet classification task. FLT provides **2.3%** accuracy gain. **Right:** Additional ablation studies for the FLT architecture, where number of modes T for the Gaussian mixture RPEs as well as the number of random features r used to encode the RPE varies. The red dotted line indicates the performance of the regular Performer.

- *Random feature attention* (RFA) proposed by Peng et al. (2021), which has two variants (Gaussian and arc-cosine) and an optional gating mechanism.
- The regular *Performer* proposed by Choromanski et al. (2021), which applies the FAVOR+ mechanism for attention matrix approximation.
- *Performer-SPE* proposed by Liutkus et al. (2021), which incorporates a special class of RPE into low-rank attention and has two variants (sineSPE and convSPE).
- The *log-linear Performer* proposed by Luo et al. (2021) which extends Performers to work with an arbitrary Toeplitz RPE attention mask.

Implementation details. All the tested models are efficient Transformer variants based on kernelized low-rank attention, with 6 decoder layers. In each layer, there are 8 attention heads. The hidden dimension is set to 512. The dimension of the feed-forward sub-layer is set to 2048. The feature map dimension m is set to 64 in the low-rank approximation of the attention matrix. For our FLT models, the number of random features for RPE r is set to 32. More details regarding training can be found in Appendix A.2. We use the validation perplexity as the evaluation metric: lower perplexity indicates better performances.

4.1.2. RESULTS

The results are shown in Table 1. Both variants of our FLT outperform all the baselines. Compared with efficient

Transformers without RPE, our FLT obtains much stronger performance. For example, the validation perplexity of our FLT with local RPE is 1.0 point lower than that of the regular Performer, which indicates that our method brings substantial performance gains by incorporating RPE into the attention module.

Compared with other efficient Transformer variants *with* RPE, our FLT is still very competitive. For example, our FLT achieves lower perplexity than the strong log-linear Performer baseline. Note that our FLT is also more *efficient* than the log-linear Performer. As we have noted before, the time and space complexity of the FLT are $O(L(m+r)d)$ and $O(L(m+r) + (m+r)d + Ld)$, respectively, while the time and space complexity of log-linear Performer are $O(Lmd \log L)$ and $O(Lmd)$. Therefore, our FLT is both more accurate and more scalable than the baselines.

4.2. Image classification

We thoroughly benchmarked FLT variants of Vision Transformers (ViTs, Dosovitskiy et al., 2021) on several image classification datasets, see Table 2.

4.2.1. COMPARED METHODS

We compared FLT with the regular Performer and its variations incorporating different methods for efficient RPE-masking. We chose our most competitive competitor from Sec. 4.1, the *log-linear Performer*, and added the *Factor-Performer* variant based on the matrix approximation frame-

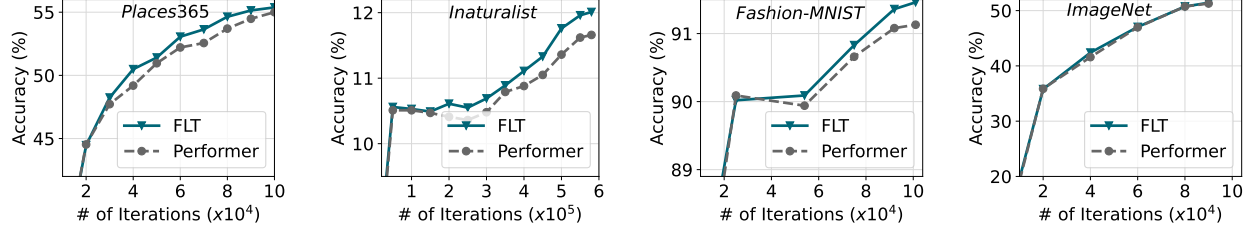


Figure 3. Comparison of the FLT with a regular Performer on different classification datasets: Places365, Inaturalist, Fashion-MNIST and ImageNet, but with the Transformer topology from (Dehghani et al., 2019) (as opposed to Fig. 2).

Dataset name	ImageNet2012	Places365	Inaturalist2021	Fashion-MNIST
Performer training time	6h 22 min	6h 41 min	7h 28 min	56 min
FLT training time	6h 28 min	8h 23 min	6h 43 min	55 min
Performer # steps / sec	5.331	5.283	27.38	33.18
FLT # steps / sec	4.625	4.586	28.38	33.93

Table 3. Comparisons of the total train time and number of steps per second for the FLT and Performer architecture on four classification datasets. Total train time includes also preemptions periods and thus is not as accurate metric as the number of steps per second (we report it for completeness though). We highlighted in **bold** the faster architecture. All the experiments were run on the TPU architecture.

work from (Halko et al., 2011). The latter first approximates the action-space of a matrix \mathbf{N} by applying random Gaussian vectors to probe it (such a probing can be done efficiently without explicitly materializing \mathbf{N} since \mathbf{N} in this setting is Toeplitz and admits log-linear matrix-vector multiplication) and then computes its orthonormal basis to use for the low-rank decomposition of \mathbf{N} .

Implementation details. All tested ViTs consist of 12 layers with 12 attention heads in each layer. The dimension of the feed-forward sub-layer is set to 3072. More details regarding training can be found in Appendix A.2.

The regular Performer baseline applies the FAVOR+ mechanism from (Choromanski et al., 2021) for attention matrix approximation with $m = 128$ random features and resampling mechanism turned off. The FLT variant uses the same core attention mechanism and applies Gaussian mixture RPEs (Sec. 3.3) with T varying between 6 and 50, and the number of random features for RPE-encoding $r = 64$. In addition, we run more detailed ablation studies on T and r for the ImageNet dataset.

4.2.2. RESULTS

The results are presented in Figs. 2 and 3. The log-linear Performer architecture ran out of memory for $m = 128$ and did not train when m was reduced (with a fixed batch size of 4096) to fit the assigned memory. The Factor-Performer variant did not exceed the allocated memory, but also did not train due to the numerical instability of the Gram-Schmidt orthogonalization procedure applied to find an orthonormal basis of the action-space of \mathbf{N} . Hence these variants are

not presented on the plots.

For the ImageNet classification task, FLT provided a 2.3% accuracy improvement over regular Performer with the number of Gaussian mixture modes $T = 25$ and the number of random features for RPE $r = 64$ (Fig. 2). Additional ablations over T and r demonstrated that increasing r improves accuracy, but more interestingly, this does not need to be the case when T is increased. In fact the best FLT variant used only $T = 25$ Gaussian modes and was substantially better than its counterpart with $T = 50$ (and the same $r = 64$). This suggests that even though increasing T also increases model expressiveness, it might make training more difficult.

Fig. 3 shows that FLT provides improvements also on other datasets, though the gains vary. We also present there the performance of FLT, as compared to the Performer, on the ImageNet dataset, but for the modified ViT model, the so-called *Universal Transformer* (Dehghani et al., 2019).

In all the experiments from Fig. 3 we applied at most $T = 50$ Gaussian modes - a negligible overhead in terms of the total number of parameters of the architecture.

The comparison of the training time of the regular Performer and the FLT architecture on all considered image datasets as well as the number of Transformer steps per second for both architectures is presented in Table 3. Total training time includes the preemption periods that are not related to the time complexity of the mechanism. We see that in practice FLT has speed comparable to the regular Performer and in fact is faster on two out of four datasets.

4.3. Molecular property prediction

We further evaluate our FLT model on the molecular property prediction task to show its capability to handle 3D input data and complicated (non-Toeplitz) RPE-masks. To the best of our knowledge, in this scenario, FLT is the *first* Transformer providing RPE-enhanced scalable attention that enjoys *linear* complexity with respect to the number of input tokens.

We use a publicly-available large-scale electrocatalysts dataset - the Open Catalyst 2020 (OC20) dataset and focus on the IS2RE task which requires to predict the energy of the relaxed structure given the initial structure of solid catalysts with adsorbate molecules (Chanussot* et al., 2021).

4.3.1. COMPARED METHODS

We compare our FLT with the regular Performer without RPE. For the FLT model, we consider to approximate RPE-masks based on Gaussian basis functions, which are popularly used in neural networks for molecular modeling (Gasteiger et al., 2021; Shi et al., 2022; Luo et al., 2022a). Specifically, the RPE-mask is defined as $\mathbf{N} = [f(\mathbf{r}_i - \mathbf{r}_j)]_{i,j=1,\dots,L} \in \mathbb{R}^{L \times L}$, where $\mathbf{r}_i \in \mathbb{R}^3$ is the position of the i -th input atom, L is the total number of input atom, and $f(\mathbf{r}) = \sum_{t=1}^T \frac{w_t}{(\sqrt{2\pi}\sigma_t)^3} \exp\left(-\frac{\|\mathbf{r}\|^2}{2\sigma_t^2}\right)$. Note that RPE only calculates the relative distances between atoms, which naturally preserves many invariant and equivariant properties. It is easy to see that the Fourier Transform of f is $g_f(\xi) = \sum_{t=1}^T w_t \exp(-2\pi^2\sigma_t^2\|\xi\|^2)$, which enables us to approximate the RPE-mask \mathbf{N} in FLTs using the technique described in Sec. 3.

Implementation details. We adopt most of the hyperparameters and training recipes of 3D-Graphomer (Shi et al., 2022). Specifically, we trained a regular Performer with 12 layers and two FLT with 10 and 12 layers respectively. Following existing works (Jumper et al., 2021; Shi et al., 2022), model outputs are repeatedly fed to the model for four times. In each layer, there are 48 attention heads. The hidden dimension is set to 768. The dimension of the feed-forward sub-layer is set to 2048. The feature map dimension m is set to 64 in the low-rank approximation of the attention matrix. For our FLT models, the number of random features for RPE r is set to 16 and the number of Gaussian basis functions in RPE T is set to 32. More details can be found in Appendix A.2.

We evaluate the performance of the tested models on the in-domain validation set, where the validation samples come from the same distribution as the training distribution. We use Mean Absolute Error (MAE) of the energies and the percentage of Energies within a Threshold (EwT) of the ground truth energy to evaluate the accuracy of the pre-

	Energy MAE (eV)	EwT (%)
Performer-12L	0.5454	4.90
FLT-10L (ours)	0.5157	5.44
FLT-12L (ours)	0.5046	5.33

Table 4. Comparisons of the FLT with the regular Performer on OC20 IS2RE task. The suffix “- k L” means the model consists of k layers, e.g., FLT-10L refers to a 10-layer FLT. The evaluation metrics are Mean Absolute Error (MAE) of the energies and the percentage of Energies within a Threshold (EwT) of the ground truth energy. We highlighted in **bold** the best performance.

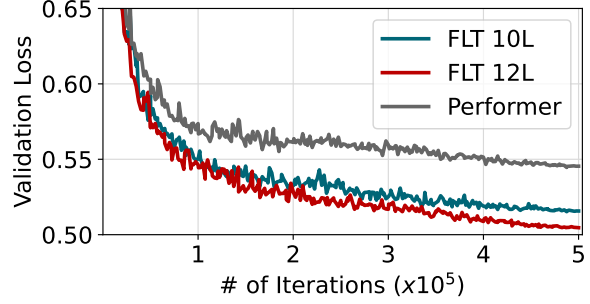


Figure 4. Validation loss curves of FLTs and the regular Performer on the IS2RE task of OC20 dataset.

dicted energies.

4.3.2. RESULTS

The results are presented in Table 4. We also present the validation loss curves of the models in Fig. 4 for a more comprehensive comparison. Clearly, our FLT models obtain better performance in both evaluation metrics and produce more accurate energy predictions. For example, the energy MAE of the 12-layer FLT is more than 0.04eV lower than that of the 12-layer regular Performer, which indicates that the use of RPE effectively increases the predictive power of the model. One may argue that the use of RPE in FLT may add some computational overhead and increase the number of model parameters. However, it should be noted that a shallower 10-layer FLT can also significantly outperform the 12-layer regular Performer, while being faster and using less parameters. Therefore, we believe our FLT is a powerful scalable Transformer variant for 3D data with complex RPE.

5. Conclusion

We introduced a new class of Transformers called FourierLearner-Transformers (FLTs) that effectively adapt the relative positional encoding (RPE) mechanism into Performers - low-rank implicit-attention Transformers with linear space and time complexity. In contrast to other architectures combining Performers with RPEs, FLTs maintain linear complexity of the attention modules with no additional structural assumptions regarding the RPE-mask.

FLTs allow the use of certain structural inductive bias techniques to specify masking strategies, e.g. they provide a way to learn local RPEs and inject locality bias. We thoroughly tested FLTs on various tasks and data modalities, including language modeling, image classification and 3D molecular property prediction. For certain modalities, such as 3D data, they are (to the best of our knowledge) the first Transformers providing linear attention and including RPE-masking.

References

Borgeaud, S., Mensch, A., Hoffmann, J., Cai, T., Rutherford, E., Millican, K., van den Driessche, G., Lespiau, J., Damoc, B., Clark, A., de Las Casas, D., Guy, A., Menick, J., Ring, R., Hennigan, T., Huang, S., Maggiore, L., Jones, C., Cassirer, A., Brock, A., Paganini, M., Irving, G., Vinyals, O., Osindero, S., Simonyan, K., Rae, J. W., Elsen, E., and Sifre, L. Improving language models by retrieving from trillions of tokens. In Chaudhuri, K., Jegelka, S., Song, L., Szepesvári, C., Niu, G., and Sabato, S. (eds.), *International Conference on Machine Learning, ICML 2022, 17-23 July 2022, Baltimore, Maryland, USA*, volume 162 of *Proceedings of Machine Learning Research*, pp. 2206–2240. PMLR, 2022. URL <https://proceedings.mlr.press/v162/borgeaud22a.html>.

Brown, T. B., Mann, B., Ryder, N., Subbiah, M., Kaplan, J., Dhariwal, P., Neelakantan, A., Shyam, P., Sastry, G., Askell, A., Agarwal, S., Herbert-Voss, A., Krueger, G., Henighan, T., Child, R., Ramesh, A., Ziegler, D. M., Wu, J., Winter, C., Hesse, C., Chen, M., Sigler, E., Litwin, M., Gray, S., Chess, B., Clark, J., Berner, C., McCandlish, S., Radford, A., Sutskever, I., and Amodei, D. Language models are few-shot learners. *CoRR*, abs/2005.14165, 2020. URL <https://arxiv.org/abs/2005.14165>.

Chanussot*, L., Das*, A., Goyal*, S., Lavril*, T., Shuaibi*, M., Riviere, M., Tran, K., Heras-Domingo, J., Ho, C., Hu, W., Palizhati, A., Sriram, A., Wood, B., Yoon, J., Parikh, D., Zitnick, C. L., and Ulissi, Z. Open catalyst 2020 (oc20) dataset and community challenges. *ACS Catalysis*, 2021. doi: 10.1021/acscatal.0c04525.

Choromanski, K., Lin, H., Chen, H., Zhang, T., Sehanobish, A., Likhosherstov, V., Parker-Holder, J., Sarlós, T., Weller, A., and Weingarten, T. From block-Toeplitz matrices to differential equations on graphs: towards a general theory for scalable masked transformers. In Chaudhuri, K., Jegelka, S., Song, L., Szepesvári, C., Niu, G., and Sabato, S. (eds.), *International Conference on Machine Learning, ICML 2022, 17-23 July 2022, Baltimore, Maryland, USA*, volume 162 of *Proceedings of Machine Learning Research*, pp. 3962–3983. PMLR, 2022a. URL <https://proceedings.mlr.press/v162/choromanski22a.html>.

Choromanski, K. M., Likhosherstov, V., Dohan, D., Song, X., Gane, A., Sarlós, T., Hawkins, P., Davis, J. Q., Mohiuddin, A., Kaiser, L., Belanger, D. B., Colwell, L. J., and Weller, A. Rethinking attention with performers. In *9th International Conference on Learning Representations, ICLR 2021, Virtual Event, Austria, May 3-7, 2021*. OpenReview.net, 2021. URL <https://openreview.net/forum?id=Ua6zuk0WRH>.

Choromanski, K. M., Lin, H., Chen, H., Sehanobish, A., Ma, Y., Jain, D., Varley, J., Zeng, A., Ryoo, M. S., Likhosherstov, V., Kalashnikov, D., Sindhwan, V., and Weller, A. Hybrid random features. In *The Tenth International Conference on Learning Representations, ICLR 2022, Virtual Event, April 25-29, 2022*. OpenReview.net, 2022b. URL <https://openreview.net/forum?id=EMigfE6ZeS>.

Chowdhery, A., Narang, S., Devlin, J., Bosma, M., Mishra, G., Roberts, A., Barham, P., Chung, H. W., Sutton, C., Gehrman, S., Schuh, P., Shi, K., Tsvyashchenko, S., Maynez, J., Rao, A., Barnes, P., Tay, Y., Shazeer, N., Prabhakaran, V., Reif, E., Du, N., Hutchinson, B., Pope, R., Bradbury, J., Austin, J., Isard, M., Gur-Ari, G., Yin, P., Duke, T., Levskaya, A., Ghemawat, S., Dev, S., Michalewski, H., Garcia, X., Misra, V., Robinson, K., Fedus, L., Zhou, D., Ippolito, D., Luan, D., Lim, H., Zoph, B., Spiridonov, A., Sepassi, R., Dohan, D., Agrawal, S., Omernick, M., Dai, A. M., Pillai, T. S., Pelлат, M., Lewkowycz, A., Moreira, E., Child, R., Polozov, O., Lee, K., Zhou, Z., Wang, X., Saeta, B., Diaz, M., Firat, O., Catasta, M., Wei, J., Meier-Hellstern, K., Eck, D., Dean, J., Petrov, S., and Fiedel, N. Palm: Scaling language modeling with pathways. *CoRR*, abs/2204.02311, 2022. doi: 10.48550/arXiv.2204.02311. URL <https://doi.org/10.48550/arXiv.2204.02311>.

Chowdhury, S. P., Solomou, A., Dubey, A., and Sachan, M. On learning the transformer kernel. *Transactions of Machine Learning Research*, 2022. URL <https://arxiv.org/abs/2110.08323>.

Clauwaert, J., Menschaert, G., and Waegeman, W. Explainability in transformer models for functional genomics. *Briefings Bioinform.*, 22(5), 2021. doi: 10.1093/bib/bbab060. URL <https://doi.org/10.1093/bib/bbab060>.

Dehghani, M., Gouws, S., Vinyals, O., Uszkoreit, J., and Kaiser, L. Universal transformers. In *7th International Conference on Learning Representations, ICLR 2019, New Orleans, LA, USA, May 6-9, 2019*. OpenReview.net, 2019. URL <https://openreview.net/forum?id=HyzdRiR9Y7>.

Deng, J., Dong, W., Socher, R., Li, L., Li, K., and Fei-Fei, L. Imagenet: A large-scale hierarchical image database. In *2009 IEEE Computer Society Conference on Computer Vision and Pattern Recognition (CVPR 2009), 20-25 June 2009, Miami, Florida, USA*, pp. 248–255. IEEE Computer Society, 2009. doi: 10.1109/CVPR.2009.5206848. URL <https://doi.org/10.1109/CVPR.2009.5206848>.

Devlin, J., Chang, M., Lee, K., and Toutanova, K. BERT: pre-training of deep bidirectional transformers for language understanding. In Burstein, J., Doran, C., and Solorio, T. (eds.), *Proceedings of the 2019 Conference of the North American Chapter of the Association for Computational Linguistics: Human Language Technologies, NAACL-HLT 2019, Minneapolis, MN, USA, June 2-7, 2019, Volume 1 (Long and Short Papers)*, pp. 4171–4186. Association for Computational Linguistics, 2019. doi: 10.18653/v1/n19-1423. URL <https://doi.org/10.18653/v1/n19-1423>.

Dosovitskiy, A., Beyer, L., Kolesnikov, A., Weissenborn, D., Zhai, X., Unterthiner, T., Dehghani, M., Minderer, M., Heigold, G., Gelly, S., Uszkoreit, J., and Houlsby, N. An image is worth 16x16 words: Transformers for image recognition at scale. In *9th International Conference on Learning Representations, ICLR 2021, Virtual Event, Austria, May 3-7, 2021*. OpenReview.net, 2021. URL <https://openreview.net/forum?id=YicbFdNTTy>.

Du, N., Huang, Y., Dai, A. M., Tong, S., Lepikhin, D., Xu, Y., Krikun, M., Zhou, Y., Yu, A. W., Firat, O., Zoph, B., Fedus, L., Bosma, M. P., Zhou, Z., Wang, T., Wang, Y. E., Webster, K., Pellar, M., Robinson, K., Meier-Hellstern, K. S., Duke, T., Dixon, L., Zhang, K., Le, Q. V., Wu, Y., Chen, Z., and Cui, C. Glam: Efficient scaling of language models with mixture-of-experts. In Chaudhuri, K., Jegelka, S., Song, L., Szepesvári, C., Niu, G., and Sabato, S. (eds.), *International Conference on Machine Learning, ICML 2022, 17-23 July 2022, Baltimore, Maryland, USA*, volume 162 of *Proceedings of Machine Learning Research*, pp. 5547–5569. PMLR, 2022. URL <https://proceedings.mlr.press/v162/du22c.html>.

Gasteiger, J., Becker, F., and Günnemann, S. Gemnet: Universal directional graph neural networks for molecules. *Advances in Neural Information Processing Systems*, 34: 6790–6802, 2021.

Gong, Z., Gao, C., Wang, Y., Gu, W., Peng, Y., and Xu, Z. Source code summarization with structural relative position guided transformer. In *IEEE International Conference on Software Analysis, Evolution and Reengineering, SANER 2022, Honolulu, HI, USA, March 15-18, 2022*, pp. 13–24. IEEE, 2022. doi: 10.1109/SANER53432.2022.00013. URL <https://doi.org/10.1109/SANER53432.2022.00013>.

Gupta, A. and Rush, A. Dilated convolutions for modeling long-distance genomic dependencies, 2017. URL <https://doi.org/10.1101/200857>.

Halko, N., Martinsson, P., and Tropp, J. A. Finding structure with randomness: Probabilistic algorithms for constructing approximate matrix decompositions. *SIAM Rev.*, 53(2):217–288, 2011. doi: 10.1137/090771806. URL <https://doi.org/10.1137/090771806>.

Horn, G. V., Aodha, O. M., Song, Y., Cui, Y., Sun, C., Shepard, A., Adam, H., Perona, P., and Belongie, S. J. The inaturalist species classification and detection dataset. In *2018 IEEE Conference on Computer Vision and Pattern Recognition, CVPR 2018, Salt Lake City, UT, USA, June 18-22, 2018*, pp. 8769–8778. Computer Vision Foundation / IEEE Computer Society, 2018. doi: 10.1109/CVPR.2018.00914. URL http://openaccess.thecvf.com/content_cvpr_2018/html/Van_Horn_The_INaturalist_Species_CVPR_2018_paper.html.

Horn, M., Shridhar, K., Groenewald, E., and Baumann, P. F. M. Translational equivariance in kernelizable attention. *CoRR*, abs/2102.07680, 2021. URL <https://arxiv.org/abs/2102.07680>.

Ji, Y., Zhou, Z., Liu, H., and Davuluri, R. V. DNABERT: pre-trained bidirectional encoder representations from transformers model for dna-language in genome. *Bioinform.*, 37(15):2112–2120, 2021. doi: 10.1093/bioinformatics/btab083. URL <https://doi.org/10.1093/bioinformatics/btab083>.

Jumper, J., Evans, R., Pritzel, A., Green, T., Figurnov, M., Ronneberger, O., Tunyasuvunakool, K., Bates, R., Žídek, A., Potapenko, A., et al. Highly accurate protein structure prediction with alphafold. *Nature*, 596(7873):583–589, 2021.

Katharopoulos, A., Vyas, A., Pappas, N., and Fleuret, F. Transformers are rnns: Fast autoregressive transformers with linear attention. In *International Conference on Machine Learning*, pp. 5156–5165. PMLR, 2020.

Kitaev, N., Kaiser, L., and Levskaya, A. Reformer: The efficient transformer. In *8th International Conference on Learning Representations, ICLR 2020, Addis Ababa, Ethiopia, April 26-30, 2020*. OpenReview.net, 2020. URL <https://openreview.net/forum?id=rkgNKkHtvB>.

Lan, Z., Chen, M., Goodman, S., Gimpel, K., Sharma, P., and Soricut, R. ALBERT: A lite BERT for self-supervised

learning of language representations. In *8th International Conference on Learning Representations, ICLR 2020, Addis Ababa, Ethiopia, April 26-30, 2020*. OpenReview.net, 2020. URL <https://openreview.net/forum?id=H1eA7AEtvS>.

Lewkowycz, A., Andreassen, A., Dohan, D., Dyer, E., Michalewski, H., Ramasesh, V. V., Slone, A., Anil, C., Schlag, I., Gutman-Solo, T., Wu, Y., Neyshabur, B., Gur-Ari, G., and Misra, V. Solving quantitative reasoning problems with language models. *CoRR*, abs/2206.14858, 2022. doi: 10.48550/arXiv.2206.14858. URL <https://doi.org/10.48550/arXiv.2206.14858>.

Likhosherstov, V., Choromanski, K., Dubey, A., Liu, F., Sarlós, T., and Weller, A. Chefs' random tables: Non-trigonometric random features. *to appear at AAAI 2023*, abs/2205.15317, 2022. doi: 10.48550/arXiv.2205.15317. URL <https://doi.org/10.48550/arXiv.2205.15317>.

Liu, Y., Ott, M., Goyal, N., Du, J., Joshi, M., Chen, D., Levy, O., Lewis, M., Zettlemoyer, L., and Stoyanov, V. Roberta: A robustly optimized BERT pretraining approach. *CoRR*, abs/1907.11692, 2019. URL <http://arxiv.org/abs/1907.11692>.

Liutkus, A., Cífká, O., Wu, S., Simsekli, U., Yang, Y., and Richard, G. Relative positional encoding for transformers with linear complexity. In Meila, M. and Zhang, T. (eds.), *Proceedings of the 38th International Conference on Machine Learning, ICML 2021, 18-24 July 2021, Virtual Event*, volume 139 of *Proceedings of Machine Learning Research*, pp. 7067–7079. PMLR, 2021. URL <http://proceedings.mlr.press/v139/liutkus21a.html>.

Luo, S., Li, S., Cai, T., He, D., Peng, D., Zheng, S., Ke, G., Wang, L., and Liu, T. Stable, fast and accurate: Kernelized attention with relative positional encoding. *CoRR*, abs/2106.12566, 2021. URL <https://arxiv.org/abs/2106.12566>.

Luo, S., Chen, T., Xu, Y., Zheng, S., Liu, T.-Y., Wang, L., and He, D. One transformer can understand both 2d & 3d molecular data. *arXiv preprint arXiv:2210.01765*, 2022a.

Luo, S., Li, S., Zheng, S., Liu, T.-Y., Wang, L., and He, D. Your transformer may not be as powerful as you expect. *arXiv preprint arXiv:2205.13401*, 2022b.

Ouyang, L., Wu, J., Jiang, X., Almeida, D., Wainwright, C. L., Mishkin, P., Zhang, C., Agarwal, S., Slama, K., Ray, A., Schulman, J., Hilton, J., Kelton, F., Miller, L., Simens, M., Askell, A., Welinder, P., Christiano, P. F., Leike, J., and Lowe, R. Training language models to follow instructions with human feedback. *CoRR*, abs/2203.02155, 2022. doi: 10.48550/arXiv.2203.02155. URL <https://doi.org/10.48550/arXiv.2203.02155>.

Peng, H., Pappas, N., Yogatama, D., Schwartz, R., Smith, N., and Kong, L. Random feature attention. In *International Conference on Learning Representations*, 2021. URL <https://openreview.net/forum?id=QtTKTdVrFBB>.

Radford, A. and Narasimhan, K. Improving language understanding by generative pre-training. 2018.

Rae, J. W., Borgeaud, S., Cai, T., Millican, K., Hoffmann, J., Song, H. F., Aslanides, J., Henderson, S., Ring, R., Young, S., Rutherford, E., Hennigan, T., Menick, J., Cassirer, A., Powell, R., van den Driessche, G., Hendricks, L. A., Rauh, M., Huang, P., Glaese, A., Welbl, J., Dathathri, S., Huang, S., Uesato, J., Mellor, J., Higgins, I., Creswell, A., McAleese, N., Wu, A., Elsen, E., Jayakumar, S. M., Buchatskaya, E., Budden, D., Sutherland, E., Simonyan, K., Paganini, M., Sifre, L., Martens, L., Li, X. L., Kunccoro, A., Nematzadeh, A., Gribovskaya, E., Donato, D., Lazaridou, A., Mensch, A., Lespiau, J., Tsimpoukelli, M., Grigorev, N., Fritz, D., Sottiaux, T., Pajarskas, M., Pohlen, T., Gong, Z., Toyama, D., de Masson d'Autume, C., Li, Y., Terzi, T., Mikulik, V., Babuschkin, I., Clark, A., de Las Casas, D., Guy, A., Jones, C., Bradbury, J., Johnson, M., Hechtman, B. A., Weidinger, L., Gabriel, I., Isaac, W. S., Lockhart, E., Osindero, S., Rimell, L., Dyer, C., Vinyals, O., Ayoub, K., Stanway, J., Bennett, L., Hassabis, D., Kavukcuoglu, K., and Irving, G. Scaling language models: Methods, analysis & insights from training gopher. *CoRR*, abs/2112.11446, 2021. URL <https://arxiv.org/abs/2112.11446>.

Raffel, C., Shazeer, N., Roberts, A., Lee, K., Narang, S., Matena, M., Zhou, Y., Li, W., and Liu, P. J. Exploring the limits of transfer learning with a unified text-to-text transformer. *J. Mach. Learn. Res.*, 21:140:1–140:67, 2020. URL <http://jmlr.org/papers/v21/20-074.html>.

Rahimi, A. and Recht, B. Random features for large-scale kernel machines. In Platt, J. C., Koller, D., Singer, Y., and Roweis, S. T. (eds.), *Advances in Neural Information Processing Systems 20, Proceedings of the Twenty-First Annual Conference on Neural Information Processing Systems, Vancouver, British Columbia, Canada, December 3-6, 2007*, pp. 1177–1184. Curran Associates, Inc., 2007.

Ramesh, A., Pavlov, M., Goh, G., Gray, S., Voss, C., Radford, A., Chen, M., and Sutskever, I. Zero-shot text-to-image generation. In Meila, M. and Zhang, T. (eds.), *Proceedings of the 38th International Conference on Machine Learning, ICML 2021, 18-24 July 2021, Virtual Event*, volume 139 of *Proceedings of Machine Learning Research*, pp. 7067–7079. PMLR, 2021. URL <http://proceedings.mlr.press/v139/ramesh21a.html>.

2021, *Virtual Event*, volume 139 of *Proceedings of Machine Learning Research*, pp. 8821–8831. PMLR, 2021. URL <http://proceedings.mlr.press/v139/ramesh21a.html>.

Reed, S. E., Zolna, K., Parisotto, E., Colmenarejo, S. G., Novikov, A., Barth-Maron, G., Gimenez, M., Sulsky, Y., Kay, J., Springenberg, J. T., Eccles, T., Bruce, J., Razavi, A., Edwards, A., Heess, N., Chen, Y., Hadsell, R., Vinyals, O., Bordbar, M., and de Freitas, N. A generalist agent. *CoRR*, abs/2205.06175, 2022. doi: 10.48550/arXiv.2205.06175. URL <https://doi.org/10.48550/arXiv.2205.06175>.

Roy, A., Saffar, M., Vaswani, A., and Grangier, D. Efficient content-based sparse attention with routing transformers. *Trans. Assoc. Comput. Linguistics*, 9:53–68, 2021. URL <https://transacl.org/ojs/index.php/tacl/article/view/2405>.

Shaw, P., Uszkoreit, J., and Vaswani, A. Self-attention with relative position representations. In Walker, M. A., Ji, H., and Stent, A. (eds.), *Proceedings of the 2018 Conference of the North American Chapter of the Association for Computational Linguistics: Human Language Technologies, NAACL-HLT, New Orleans, Louisiana, USA, June 1-6, 2018, Volume 2 (Short Papers)*, pp. 464–468. Association for Computational Linguistics, 2018. doi: 10.18653/v1/n18-2074. URL <https://doi.org/10.18653/v1/n18-2074>.

Shi, Y., Zheng, S., Ke, G., Shen, Y., You, J., He, J., Luo, S., Liu, C., He, D., and Liu, T.-Y. Benchmarking graphomer on large-scale molecular modeling datasets. *arXiv preprint arXiv:2203.04810*, 2022.

Srivastava, A., Rastogi, A., Rao, A., Shoeb, A. A. M., Abid, A., Fisch, A., Brown, A. R., Santoro, A., Gupta, A., Garriga-Alonso, A., Kluska, A., Lewkowycz, A., Agarwal, A., Power, A., Ray, A., Warstadt, A., Kocurek, A. W., Safaya, A., Tazarv, A., Xiang, A., Parish, A., Nie, A., Hussain, A., Askell, A., Dsouza, A., Rahane, A., Iyer, A. S., Andreassen, A., Santilli, A., Stuhlmüller, A., Dai, A. M., La, A., Lampinen, A. K., Zou, A., Jiang, A., Chen, A., Vuong, A., Gupta, A., Gottardi, A., Norelli, A., Venkatesh, A., Gholamidavoodi, A., Tabassum, A., Menezes, A., Kirubarajan, A., Mulkandov, A., Sabharwal, A., Herrick, A., Efrat, A., Erdem, A., Karakas, A., and et al. Beyond the imitation game: Quantifying and extrapolating the capabilities of language models. *CoRR*, abs/2206.04615, 2022. doi: 10.48550/arXiv.2206.04615. URL <https://doi.org/10.48550/arXiv.2206.04615>.

Sun, Z., Yang, Y., and Yoo, S. Sparse attention with learning to hash. In *The Tenth International Conference on Learning Representations, ICLR 2022, Virtual Event, April 25-29, 2022*. OpenReview.net, 2022. URL <https://openreview.net/forum?id=VGnOJhd5Q1q>.

Tay, Y., Dehghani, M., Abnar, S., Shen, Y., Bahri, D., Pham, P., Rao, J., Yang, L., Ruder, S., and Metzler, D. Long range arena : A benchmark for efficient transformers. In *9th International Conference on Learning Representations, ICLR 2021, Virtual Event, Austria, May 3-7, 2021*. OpenReview.net, 2021. URL <https://openreview.net/forum?id=qVyeW-grC2k>.

Thoppilan, R., Freitas, D. D., Hall, J., Shazeer, N., Kulshreshtha, A., Cheng, H., Jin, A., Bos, T., Baker, L., Du, Y., Li, Y., Lee, H., Zheng, H. S., Ghafouri, A., Mene-gali, M., Huang, Y., Krikun, M., Lepikhin, D., Qin, J., Chen, D., Xu, Y., Chen, Z., Roberts, A., Bosma, M., Zhou, Y., Chang, C., Krivokon, I., Rusch, W., Pickett, M., Meier-Hellstern, K. S., Morris, M. R., Doshi, T., Santos, R. D., Duke, T., Soraker, J., Zevenbergen, B., Prabhakaran, V., Diaz, M., Hutchinson, B., Olson, K., Molina, A., Hoffman-John, E., Lee, J., Aroyo, L., Rajakumar, R., Butryna, A., Lamm, M., Kuzmina, V., Fen-ton, J., Cohen, A., Bernstein, R., Kurzweil, R., Aguera-Arcas, B., Cui, C., Croak, M., Chi, E. H., and Le, Q. Lamda: Language models for dialog applications. *CoRR*, abs/2201.08239, 2022. URL <https://arxiv.org/abs/2201.08239>.

Vaswani, A., Shazeer, N., Parmar, N., Uszkoreit, J., Jones, L., Gomez, A. N., Kaiser, L., and Polosukhin, I. Attention is all you need. In Guyon, I., von Luxburg, U., Bengio, S., Wallach, H. M., Fergus, R., Vishwanathan, S. V. N., and Garnett, R. (eds.), *Advances in Neural Information Processing Systems 30: Annual Conference on Neural Information Processing Systems 2017, December 4-9, 2017, Long Beach, CA, USA*, pp. 5998–6008, 2017.

Vaswani, A., Ramachandran, P., Srinivas, A., Parmar, N., Hechtman, B. A., and Shlens, J. Scaling local self-attention for parameter efficient visual backbones. In *IEEE Conference on Computer Vision and Pattern Recognition, CVPR 2021, virtual, June 19-25, 2021*, pp. 12894–12904. Computer Vision Foundation / IEEE, 2021a. doi: 10.1109/CVPR46437.2021.01270.

Vaswani, A., Ramachandran, P., Srinivas, A., Parmar, N., Hechtman, B. A., and Shlens, J. Scaling local self-attention for parameter efficient visual backbones. In *IEEE Conference on Computer Vision and Pattern Recognition, CVPR 2021, virtual, June 19-25, 2021*, pp. 12894–12904. Computer Vision Foundation / IEEE, 2021b. URL https://openaccess.thecvf.com/content/CVPR2021/html/Vaswani_Scaling_Local_Self-Attention_for_

Parameter_Efficient_Visual_Backbones_CVPR_2021_paper.html.

Vyas, A., Katharopoulos, A., and Fleuret, F. Fast transformers with clustered attention. In Larochelle, H., Ranzato, M., Hadsell, R., Balcan, M., and Lin, H. (eds.), *Advances in Neural Information Processing Systems 33: Annual Conference on Neural Information Processing Systems 2020, NeurIPS 2020, December 6-12, 2020, virtual*, 2020. URL <https://proceedings.neurips.cc/paper/2020/hash/f6a8dd1c954c8506aadc764cc32b895e-Abstract.html>.

Wu, K., Peng, H., Chen, M., Fu, J., and Chao, H. Rethinking and improving relative position encoding for vision transformer. In *2021 IEEE/CVF International Conference on Computer Vision, ICCV 2021, Montreal, QC, Canada, October 10-17, 2021*, pp. 10013–10021. IEEE, 2021. doi: 10.1109/ICCV48922.2021.00988. URL <https://doi.org/10.1109/ICCV48922.2021.00988>.

Xiao, H., Rasul, K., and Vollgraf, R. Fashion-mnist: a novel image dataset for benchmarking machine learning algorithms. *CoRR*, abs/1708.07747, 2017. URL <http://arxiv.org/abs/1708.07747>.

Xiao, X., Zhang, T., Choromanski, K., Lee, T. E., Francis, A. G., Varley, J., Tu, S., Singh, S., Xu, P., Xia, F., Persson, S. M., Kalashnikov, D., Takayama, L., Frostig, R., Tan, J., Parada, C., and Sindhwani, V. Learning model predictive controllers with real-time attention for real-world navigation. *CoRL 2022*, abs/2209.10780, 2022. doi: 10.48550/arXiv.2209.10780. URL <https://doi.org/10.48550/arXiv.2209.10780>.

Yuan, L., Chen, Y., Wang, T., Yu, W., Shi, Y., Jiang, Z., Tay, F. E. H., Feng, J., and Yan, S. Tokens-to-token vit: Training vision transformers from scratch on imagenet. In *2021 IEEE/CVF International Conference on Computer Vision, ICCV 2021, Montreal, QC, Canada, October 10-17, 2021*, pp. 538–547. IEEE, 2021. doi: 10.1109/ICCV48922.2021.00060. URL <https://doi.org/10.1109/ICCV48922.2021.00060>.

Zaheer, M., Guruganesh, G., Dubey, K. A., Ainslie, J., Alberti, C., Ontanon, S., Pham, P., Ravula, A., Wang, Q., Yang, L., et al. Big bird: Transformers for longer sequences. *Advances in Neural Information Processing Systems*, 33:17283–17297, 2020.

Zhou, B., Lapedriza, A., Khosla, A., Oliva, A., and Torralba, A. Places: A 10 million image database for scene recognition. *IEEE Trans. Pattern Anal. Mach. Intell.*, 40(6):1452–1464, 2018. doi: 10.1109/TPAMI.2017.2723009. URL <https://doi.org/10.1109/TPAMI.2017.2723009>.

Zhou, J., Wang, P., Wang, F., Liu, Q., Li, H., and Jin, R. ELSA: enhanced local self-attention for vision transformer. *CoRR*, abs/2112.12786, 2021. URL <https://arxiv.org/abs/2112.12786>.

Žiga Avsec, Agarwal, V., Visentin, D., Ledsam, J. R., Grabska-Barwinska, A., Taylor, K. R., Assael, Y., Jumper, J. M., Kohli, P., and Kelley, D. R. Effective gene expression prediction from sequence by integrating long-range interactions. *Nature Methods*, 18:1196 – 1203, 2021.

A. Appendix

A.1. Potential negative social impact & limitations

This paper works on building scalable and powerful Transformer variants. While they led to significant advances in language modeling and several other domains, we note that they should be used cautiously, given the carbon emission footprint of their training. In addition, this paper only studies scalable Transformer variants based on low-rank attention (e.g., Performer), and the technique may not be directly applied to other classes of efficient Transformers.

A.2. Detailed experiment settings

Language modeling. Following existing works (Peng et al., 2021; Luo et al., 2021), the sequence length is set to 512 during both training and evaluation. All models are trained *without* access to the context from previous mini-batches for a fair comparison. The dropout ratio and weight decay are set to 0.1 and 0.01, respectively. The batch size is set to 64. We use Adam as the optimizer, and set its hyperparameter ε to $1e-6$ and (β_1, β_2) to $(0.9, 0.98)$. The model is trained for 150k steps with a 6k-step warm-up stage followed by an inverse square-root learning rate scheduler, with the peak learning rate set to $2e-3$.

For the FLT variant with Gaussian mixture RPE, the FT of the RPE function, i.e., the function g , is parameterized as described in Eq. (6). For the FLT variant with local RPE, the function g is parameterized as

$$g(\xi) = \sum_{t=1}^T w_t \cdot \frac{\sin(2\pi v_t \xi)}{\pi \xi}, \quad (13)$$

where w_1, \dots, w_T and v_1, \dots, v_T are learnable parameters and T is a pre-defined hyper-parameter. In this case, the underlying implicit RPE function f is

$$f(\Delta r) = \sum_{t=1}^T w_t \cdot \mathbb{1}[|\Delta r| \leq v_t]. \quad (14)$$

For both FLT variants, the RPE masks are different in different attention heads, but are *shared* across different layers. The random features ξ_1, \dots, ξ_r are sampled from the standard Gaussian distribution.

Image classification. For all the models, we used a dropout rate of 0.1 and no attention dropout. We applied the Adam optimizer with weight decay equal to 0.05 and a standard batch size of 4096. All Transformers were trained on TPU architectures until convergence.

Table 5. Hyperparameters for Image Classification.

Parameter	Value
Batch size	4096
Optimizer	AdamW
Base Learning rate	$1.5e-4$
Weight decay	0.05
Optimizer momentum	$(\beta_1, \beta_2) = (0.9, 0.95)$
Learning rate schedule	cosine decay
Warm up epochs	40
Augmentation	RandomResizedCrop
Compute resources	8×8 TPUs

Molecular property prediction. For all the models, the attention dropout ratio and the weight decay are set to 0.1 and 0.001, respectively. The batch size is set to 64. We use Adam as the optimizer, and set its hyperparameter ε to $1e-6$ and (β_1, β_2) to $(0.9, 0.98)$. The peak learning rate is set to $3e-4$ with a 10K-step warm-up stage. After the warm-up stage, the learning rate decays linearly to zero. All the models are trained for 500k steps in total.